CHEMISTRY OF MATERIALS

Communication

pubs.acs.org/cm

# Single-Nanometer-Sized Low-Valence Metal Hydroxide Crystals: Synthesis via Epoxide-Mediated Alkalinization and Assembly toward Functional Mesoporous Materials

Naoki Tarutani,[†] Yasuaki Tokudome,[*,†] Matías Jobbágy,[‡] Federico A. Viva,[§] Galo J. A. A. Soler-Illia,[#] and Masahide Takahashi[†]

[†]Department of Materials Science, Graduate School of Engineering, Osaka Prefecture University, Sakai, Osaka 599-8531, Japan

[‡]INQUIMAE-CONICET, Facultad Ciencias Exactas y Naturales, Universidad de Buenos Aires, Buenos Aires, C1428EHA, Argentina

[§]Departamento de Fisica de la Materia Condensada, Centro Atómico Constituyentes, Comisión Nacional de Energía Atómica, San Martín, B1650KNA, Argentina

[#]Instituto de Nanosistemas, Universidad Nacional de General San Martín, Av. 25 de Mayo y Francia, San Martín, 1650, Argentina

Supporting Information

Metal oxides of low-valence metal cations (M(II) and M(III); M = Al, Cr, Mn, Fe, Co, Ni, Cu, etc.) are essential in catalysis, sustainable energy, information technology, and environmental applications. In addition, the corresponding metal hydroxides present a 2D crystalline structure of hydroxide layers and interlayer anions and have attracted attention due to their properties, such as reversible and fast intercalation, deintercalation, and anisotropic transfer of ions.[1,2] The wide variety of combination of the metal cations composing the 2D hydroxide layers and the interlayer anions leads to enhanced electrochemical,[3] magnetic,[4] optical,[5] and catalytic[6] properties. These phases in turn can be transformed into other layered phases such as sulfides that present interesting electronic properties.[7]

In order to fully exploit the surface and bulk properties dictated by the nano-/mesostructure of these low-valence phases, it is desirable to process them as materials with highly accessible surface, controlled morphology, and tailored crystallite size. The possibility of shaping mesoporous metal oxides and hydroxides with high specific surface area, controlled pore size, and tunable surface functionality is particularly interesting in this framework.[8,9]

Although considerable progress has been made in the controlled synthesis of mesoporous silica and nonsilica oxides, a limitation exists in the access to mesoporous low-valence metal oxides, hydroxides, and derived phases. To date, only very few synthetic paths are reported, and the mesostructures obtained are seldom robust.[10] The difficulty of obtaining these phases can be traced back to the condensation chemistry of M(II)/M(III) centers, which present very fast crystallization and aggregation, and therefore hinder the coassembly with supramolecular templates. These strategies rely mostly on the use of hard templates or on obtaining textural porosity derived from interparticle spaces.[11] An alternative way to obtain highly ordered mesoporous phases is the use of preformed fine nanoparticles with high controllability in single-nanometer scale.[12,13] Nanoparticles presenting a given crystalline phase and well-defined shape can coassemble with the supramolecular templates as nanobuilding blocks (NBBs), avoiding the lengthy steps associated with the hard template approach. However, the synthesis of single-nanometer-sized crystals of layered metal hydroxides and their use as NBBs remain a considerable challenge. In general, a low degree of supersaturation is favored for synthesizing hydroxides to avoid aggregation, yielding coarse crystals whose size is too large to be used as NBBs. Quite recently, we reported the synthesis of nanometric Ni(II)−Al(III)-type layered double hydroxide (LDH).[14] The reaction successfully yielded 5 nm LDH which could be used as a NBB of mesoporous LDH, whereas Al(III) was found to be a mandatory element therein to achieve the developed reaction scheme involving a gelation−deflocculation transition. It still remains a challenge to achieve a chemically versatile synthesis of hydroxide NBBs made of desired cationic species.

Herein, we demonstrate a simple synthesis approach toward single-nanometer-sized crystals that work as NBBs to form a great variety of mesoporous hydroxides and derived phases. The nanocrystals with diverse chemical compositions (layered low-valence metal hydroxides, $\alpha$-M(OH)$_2$ (M = Mn(II), Fe(II), Co(II), Ni(II), and Cu(II)), and other (hydr)oxides composed of Al(III), Cr(III), Fe(III), Zr(IV), and Sn(IV)) were prepared in an aqueous ethanol solution. The nanocrystal formation was achieved by inducing a high supersaturation via the epoxide-mediated alkalinization in a concentrated metal salt solution. A variety of carboxylic acids were used as growth controlling agents, permitting to finely control the size of low-valence metal hydroxide nanocrystals and to attain high stability against aggregation. Mesoporous hydroxide materials with nanocrystalline walls were obtained by coassembly of crystalline NBBs and F127 templates through the evaporation-induced self-assembly (EISA) process as films, xerogels, and aerosol-derived powders. Functional crystalline mesostructures with desired shape dictating chemical/physical properties have been thus successfully obtained. We discuss mesoporous $\alpha$-Ni(OH)$_2$ films as an example, in which the advantages of nanocrystalline nature and mesoporous structure were demonstrated by pesudomorphic transformations to functional phases and the improvement of pseudocapacitor performance.

Received: June 21, 2016
Revised: July 24, 2016
Published: July 25, 2016





DOI: 10.1021/acs.chemmater.6b02510
Chem. Mater. 2016, 28, 5606−5610

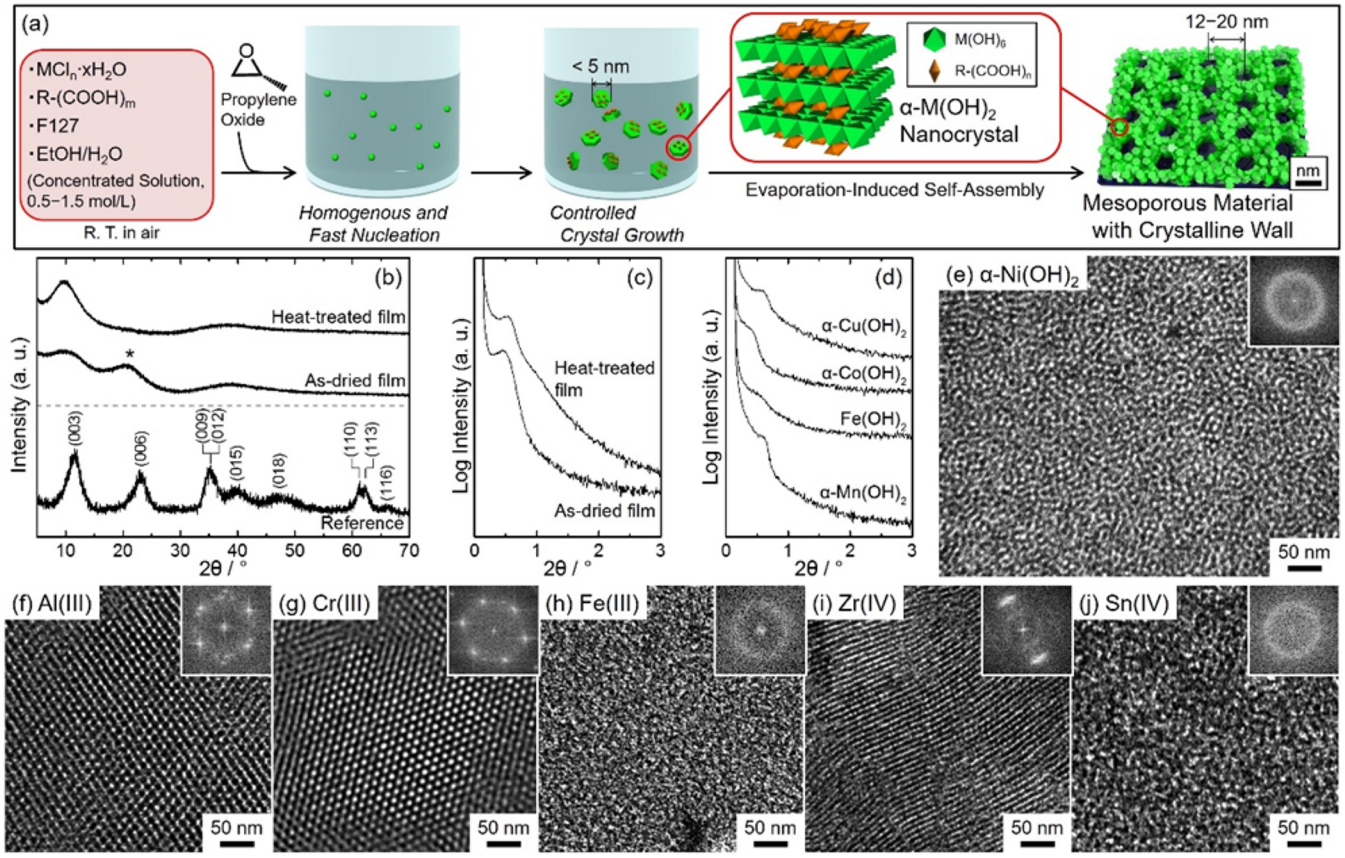


**Figure 1.** (a) Schematic illustration of our approach to prepare single-nanometer-sized nanocrystals toward mesoporous materials with crystalline walls. (b) PXRD and (c) SAXS patterns of as-dried and heat-treated (250 °C, in air) films prepared from $\alpha$-Ni(OH)$_2$ nanocrystals intercalated with $C_2H_4(COOH)_2$. The reference pattern in (b) corresponds to $C_2H_4(COOH)_2$ intercalated Ni–Al-type LDH prepared via a standard coprecipitation method. (d) SAXS patterns of as-dried films prepared from $\alpha$-M(OH)$_2$ (M = Mn(II), Fe(II), Co(II), and Cu(II)) nanocrystals intercalated with $C_3H_6(COOH)_2$. TEM images of heat-treated films prepared from (e) $\alpha$-Ni(OH)$_2$ intercalated with $C_2H_4(COOH)_2$ and (f–j) various M(III) and M(IV) (hydr)oxides nanocrystals. Heat treatment temperatures (in air): (e) 250 °C, (f–i) 350 °C. Insets of (e)–(j) are FFT patterns generated from the respective images. *Overlapped diffraction peaks derived from $\alpha$-Ni(OH)$_2$ and an impurity interstratified Ni(OH)$_2$; for more details, see Structural Assignment in Supporting Information.

Figure 1a shows a schematic illustration of the fabrication of mesoporous films with crystalline walls. The starting mixture is an aqueous ethanol solution containing metal chloride hydrate (its concentration is 5–100 times higher than those in general methods to achieve high degree of supersaturation[15]), carboxylic acid, and F127. Adding propylene oxide to the Ni-containing starting mixture results in a homogeneous and fast pH increase through the epoxide ring-opening reaction with the nucleophilic species.[16] Along with the pH increase, ionic Ni species were consumed by the nucleation and growth of $\alpha$-Ni(OH)$_2$ nanocrystals; these processes are evidenced by the decrease of electric conductivity (Figure S1a) and X-ray diffraction (XRD) of reacting solution (Figure S1b). Small angle X-ray scattering (SAXS) measurements confirmed the formation of crystals with a gyration radius of 2.6 nm (Figure S1c) which is 10-times smaller than without carboxylic acid (26.1 nm). These nanocrystals can be further used as NBBs for functional mesostructures. Upon coating, surfactant (F127) was self-assembled into ordered mesostructures[17,18] together with NBBs by the EISA process. Mesoporous thin films with hydroxide nanocrystalline walls were obtained after removal of F127.

Figure 1b shows powder XRD (PXRD) patterns of the as-dried and the heat-treated films of $\alpha$-Ni(OH)$_2$ with $C_2H_4(COOH)_2$ as a growth controlling agent. A broad peak around $2\theta = 10°$ corresponds to a $d$-spacing of 8.6 Å, which is coincident with (003) interplanar distance of Ni–Al layered double hydroxide prepared by a standard coprecipitation technique. The broad peaks indicate that the obtained film is constituted of hydroxide nanocrystals. The crystallite size along the $c$ axis, out-of-plane direction of hydroxide layers, calculated from Scherrer's equation, is less than 3 nm. The peak ascribed to the (110) plane, the in-plane direction of the hydroxide layers, was not clearly detected due to the small lateral size of the crystals. The film retained the (001) diffraction ($d_{001}$ = 8.8 Å) even after the removal of F127 by heat treatment at 250 °C (the removal of F127 was confirmed by FT-IR, see Figure S2), indicating that the obtained mesostructured $\alpha$-Ni(OH)$_2$ film was thermally stable. Figure 1c shows the SAXS patterns of the as-dried and the heat-treated films. Periodic lengths calculated from the diffraction peaks are 17.9 and 16.1 nm for the as-dried and the heat-treated films, respectively. Transmission electron microscopy (TEM) and scanning electron microscopy (SEM) confirmed a templated mesoporous structure with a well-defined pore size (Figure 1e and Figure S3). A $N_2$ adsorption/desorption isotherm of the mesoporous $\alpha$-Ni(OH)$_2$ film is classified into a typical type IV shape with a hysteresis loop of H1 (Figure S4), which is characteristic of a cylinder type mesoporous structure. The mesoporous film has a large BET specific surface area (141 m$^2$ g$^{-1}$), a large pore size (9.2 nm),


DOI: 10.1021/acs.chemmater.6b02510
Chem. Mater. 2016, 28, 5606–5610

and a large pore volume (0.30 $cm^3$ $g^{-1}$) compared to the film prepared without F127 (hereafter denoted as a nonporous film). The wall thickness of the mesostructure was calculated as 6.9 nm from the result of SAXS and $N_2$ sorption. The size of the $\alpha$-$Ni(OH)_2$ NBB is small enough compared to the wall thickness, which is the key for the synthesis of the templated mesoporous structure.

The present NBB approach is applicable to various chemical systems including low-valence metal ions, Mn(II), Fe(II), Co(II), Cu(II), Al(III), Cr(III), Fe(III), Zr(IV), and Sn(IV), yielding nanocrystals of $\alpha$-$Mn(OH)_2$, $\alpha$-$Co(OH)_2$, $Fe(OH)_2$, and $\alpha$-$Cu(OH)_2$ and trivalent and tetravalent (hydr)oxides, respectively (Figure S5a and b). SAXS patterns and TEM images confirm that the films have ordered mesostructures with periodicities ranging from 14.4 to 20.7 nm (Figure 1d–j, Figure S5c, and Table S1). Our approach toward mesoporous films can also be coupled with a spray drying technique. Micrometer-sized spherical particles with defined mesopores were successfully obtained by the aerosol-assisted EISA process (Figure S6). Spray drying is a high yield and scalable processing desired for industrial applications.[19]

The compositional versatility of both hydroxide and anion layers offers a considerable advantage in applications, that is, tunability of chemical and physical characteristics of hydr-(oxide) NBBs. For instance, the composition of hydroxide layers and interlayers is reported to affect capacitance of layered low-valence metal hydroxides.[3,20,21] Figure 2a shows PXRD

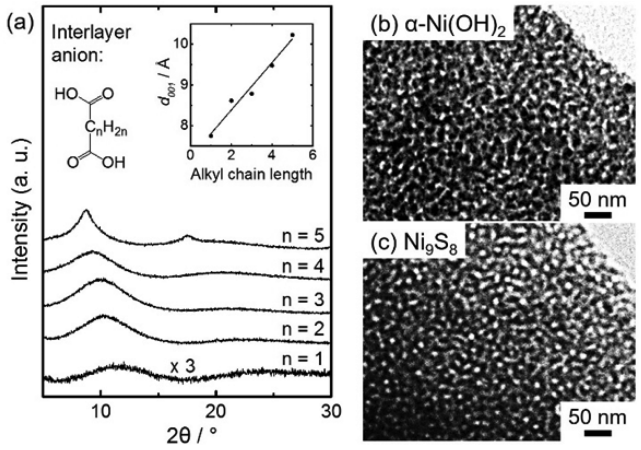


**Figure 2.** (a) PXRD patterns of films prepared from $\alpha$-$Ni(OH)_2$ NBBs intercalated with $C_nH_{2n}(COOH)_2$ ($n$ = 1–5) after the heat treatment at 250 °C in air. Inset shows $d_{001}$ vs alkyl chain length (as carbon number). TEM images of mesoporous films prepared from $\alpha$-$Ni(OH)_2$ NBB intercalated with $C_2H_3SH(COOH)_2$ (b) before and (c) after phase transformation to $Ni_9S_8$.

patterns of mesoporous films prepared from $\alpha$-$Ni(OH)_2$ NBBs intercalated with different dicarboxylic acids ($C_nH_{2n}(COOH)_2$, $n$ = 1–5). With increasing the alkyl chain length, the (001) peak shifts to lower angles. The increase of $d_{001}$ is 0.58 Å per one chain unit. Even when (001) $d$-spacing was modulated by using different carboxylic acids, mesoporous structures were successfully formed (Figure S7a–e). Various mono-, di-, and tricarboxylic acids can be intercalated in $\alpha$-$M(OH)_2$ nanocrystals which can be assembled into mesoporous structures as NBBs (Table S1). The tunability of interlayer anions as well as cationic species is a significant advance over previous reports on nanometric metal hydroxides.[14,22,23]

As Stucky and co-workers reported,[24,25] acetic acid can control the inorganic condensation of M(IV) (M = Ti, Zr, Si, and mixtures) so that inorganic species could lead to coassembly with a supramolecular template. In the present study, we found that carboxylic acids used as a growth controlling agent played multiple roles. As is evidenced by infrared spectra and XRD patterns (Figures S2 and S8a), the carboxylic acids coordinate and adsorb on the surface/edges of 2D hydroxide layers, which inhibits extensive crystal growth of hydroxide in the in-plane (110) direction.[26] This allows nanocrystals small enough for the NBB approach to form. The carboxylic acids are intercalated in the interlayer cavity as well as the crystal surface. The intercalated anionic species then can be used as chemical sources for pseudomorphic transformation as discussed later. In addition, surface carboxylic acid groups help to stabilize nanocrystals against aggregation (Figure S8b,c). The carboxylic acid is therefore indispensable to control the structural feature, as well as chemical and surface features of the $\alpha$-$M(OH)_2$ NBBs toward the formation of mesoporous structure.

Since layered hydroxides can be easily transformed to metals, oxides, and metal organic frameworks through pseudomorphic transformation,[2,27,28] the simultaneous control over the nano-/mesostructure and the chemical composition of layered hydroxide offer a versatile pathway to tune the physical and chemical properties of these materials. The obtained $\alpha$-$Ni(OH)_2$ films with a variety of interlayer anions were subjected to further heat treatments (Table S2). The interlayer anions work as chemical sources to tune the composition of the transformed phase such as NiO, Ni, Ni/$Ni_3C$, Ni/C, and $Ni_9S_8$ (Figure S9). By tuning the heat treatment condition, phase transformation was achieved without collapse of mesopore structure (Figure 2b,c). The present nanocrystals can serve as precursors for useful and functional mesoporous materials composed of crystalline walls such as $MnO_2$, $NaCoO_4$, and $Li[Mn_xCo_yNi_z]O_4$.[29–31]

As a proof-of-concept study, cyclic voltammetry (CV) and galvanostatic charge–discharge measurements were performed on the mesoporous and the nonporous $\alpha$-$Ni(OH)_2$ films. The CV curves of both $\alpha$-$Ni(OH)_2$ films show a pair of redox peaks (Figure 3a and Figure S10a,b), which is a typical feature of $Ni(OH)_2$ pseudocapacitor with Faradaic reaction of $Ni(OH)_2$ + $OH^- \leftrightarrows NiOOH + H_2O + e^-$.[32] The nonlinear galvanostatic charge–discharge curves also confirm the pseudocapacitance behavior due to quasi-reversible redox reaction (Figure 3b and

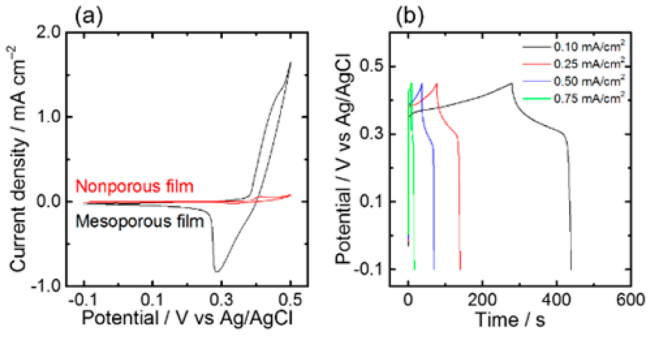


**Figure 3.** (a) CV curves of mesoporous and nonporous $\alpha$-$Ni(OH)_2$ films at a scan rate of 10 mV/s. (b) Galvanostatic charge–discharge curves of the mesoporous $\alpha$-$Ni(OH)_2$ film at various current densities. Intercalated carboxylic acid: $C_2H_4(COOH)_2$.



DOI: 10.1021/acs.chemmater.6b02510
Chem. Mater. 2016, 28, 5606–5610

Figure S10c). The area-specific capacitances calculated from the discharge curves of 0.10 mA/cm$^2$ were 29.7 and 0.176 mF/cm$^2$ for mesoporous and nonporous films, respectively. A difference of the specific surface areas of these films is only 4.4 times, which cannot account for the significant difference in the capacitances. The considerable increase of capacitance (169 times) is due to improved electrolyte mobility and high accessibility to the active sites by the introduction of mesopores of adequate size (3−10 nm).[33] The mesoporous film showed a high mass-specific capacitance (926 F/g), specific energy (31.4 Wh/kg), and specific power (3466 W/kg) at a discharge current of 14.0 A/g (Table S3). As well as the mesoporosity, the nanocrystalline nature contributes to enhancement of pseudocapacitor performance. Fabricating the $\alpha$-Ni(OH)$_2$ electrode with nanocrystals allows a high density of grain boundaries to be introduced, which is known to work as an efficient diffusion pass of electrolyte ions.[34,35] The nanocrystalline mesoporous $\alpha$-Ni(OH)$_2$ films reported here are a promising material for a high performance capacitor.

In summary, single-nanometer-sized $\alpha$-Ni(OH)$_2$ crystals in an aqueous ethanol solution were synthesized through a simple one batch process using an epoxide-mediated alkalinization with carboxylic acids. Coassembly of crystalline NBBs and supramolecular templates by EISA lead to ordered mesoporous thin films, xerogels, and aerosol-derived powders. This NBB assembly approach can be extended to other transition low- and high-valence metal ions (Mn(II), Fe(II), Co(II), Cu(II), Al(III), Cr(III), Fe(III), Zr(IV), and Sn(IV)) which were so far difficult to obtain, leading to nanocrystalline mesoporous thin films with a variety of chemical compositions. The compositional versatility enables the phase conversion from $\alpha$-Ni(OH)$_2$ to oxides, metals, metal/carbide or metal/carbon composites, and sulfides. The introduction of ordered mesopores enhanced the pseudocapacitance performance of the $\alpha$-Ni(OH)$_2$ film. The NBB approach reported here offers a promising route to obtain transition metal-based mesoporous materials/composites which are useful in a wide variety of research fields, such as catalysis, adsorbents, thermo-/chemical electric or magnetic devices, and sensing.

## ■ ASSOCIATED CONTENT

### Supporting Information

The Supporting Information is available free of charge on the ACS Publications website at DOI: 10.1021/acs.chemmater.6b02510.

Experimental details, XRD patterns, FT-IR spectra, $N_2$ sorption, SEM and TEM images, Raman spectrum, electrochemical analysis, and detailed structural assignment (PDF)

## ■ AUTHOR INFORMATION


### Corresponding Author

*(Y.T.) E-mail: tokudome@photomater.com.


### Notes

The authors declare no competing financial interest.

## ■ ACKNOWLEDGMENTS

Strategic Young Researcher Overseas Visits Program for Accelerating Brain Circulation from JSPS is gratefully acknowledged. The present work is partially supported by JSPS KAKENHI, LNLS proposal SAXS1 18927, ANPCyT (PICT 2087), the grant UBA (UBACyT 20020130100610BA), and the Foundation for the Promotion of Ion Engineering. We thank Mr. T. Morimoto for XRD measurement and Mr. S. Nikka for the helpful discussion.

## ■ REFERENCES


(1) Miyata, S. Anion-Exchange Properties of Hydrotalcite-like Compounds. *Clays Clay Miner.* **1983**, *31*, 305−311.

(2) Arizaga, G. G. C.; Satyanarayana, K. G.; Wypych, F. Layered Hydroxide Salts: Synthesis, Properties and Potential Applications. *Solid State Ionics* **2007**, *178*, 1143−1162.

(3) Tang, Y.; Liu, Y.; Yu, S.; Guo, W.; Mu, S.; Wang, H.; Zhao, Y.; Hou, L.; Fan, Y.; Gao, F. Template-Free Hydrothermal Synthesis of Nickel Cobalt Hydroxide Nanoflowers with High Performance for Asymmetric Super-Capacitor. *Electrochim. Acta* **2015**, *161*, 279−289.

(4) Taibi, M.; Jouini, N.; Rabu, P.; Ammar, S.; Fiévet, F. Lamellar Nickel Hydroxy-Halides: Anionic Exchange Synthesis, Structural Characterization and Magnetic Behavior. *J. Mater. Chem. C* **2014**, *2*, 4449−4460.

(5) Ahmed, A. A. A.; Talib, Z. A.; bin Hussein, M. Z.; Zakaria, A. Zn−Al Layered Double Hydroxide Prepared at Different Molar Ratios: Preparation, Characterization, Optical and Dielectric Properties. *J. Solid State Chem.* **2012**, *191*, 271−278.

(6) Sherman, I. T. *Layered Double Hydroxides (LDHs): Synthesis, Characterization and Applications*; Nova Science Publishers, Inc.: New York, 2015.

(7) Lee, H. S.; Min, S.-W.; Chang, Y.-G.; Park, M. K.; Nam, T.; Kim, H.; Kim, J. H.; Ryu, S.; Im, S. $MoS_2$ Nanosheet Phototransistors with Thickness-Modulated Optical Energy Gap. *Nano Lett.* **2012**, *12*, 3695−3700.

(8) Lebeau, B.; Galarneau, A.; Linden, M. Introduction for 20 Years of Research on Ordered Mesoporous Materials. *Chem. Soc. Rev.* **2013**, *42*, 3661−3662.

(9) Luque, R.; Garcia-Martinez, J. From Mesoporous Supports to Mesoporous Catalysts: Introducing Functionality to Mesoporous Materials. *ChemCatChem* **2013**, *5*, 827−829.

(10) Gu, D.; Schüth, F. Synthesis of Non-Siliceous Mesoporous Oxides. *Chem. Soc. Rev.* **2014**, *43*, 313−344.

(11) Poyraz, A. S.; Kuo, C.-H.; Biswas, S.; King'ondu, C. K.; Suib, S. L. A General Approach to Crystalline and Monomodal Pore Size Mesoporous Materials. *Nat. Commun.* **2013**, *4*, 2952.

(12) Wong, M. S.; Jeng, E. S.; Ying, J. Y. Supramolecular Templating of Thermally Stable Crystalline Mesoporous Metal Oxides Using Nanoparticulate Precursors. *Nano Lett.* **2001**, *1*, 637−642.

(13) Chane-Ching, J.-Y.; Cobo, F.; Aubert, D.; Harvey, H. G.; Airiau, M.; Corma, A. A General Method for the Synthesis of Nanostructured Large-Surface-Area Materials Through the Self-Assembly of Functionalized Nanoparticles. *Chem. - Eur. J.* **2005**, *11*, 979−987.

(14) Tokudome, Y.; Morimoto, T.; Tarutani, N.; Vaz, P. D.; Nunes, C. D.; Prevot, V.; Stenning, G. B. G.; Takahashi, M. Layered Double Hydroxide Nanoclusters: Aqueous, Concentrated, Stable, and Catalytically Active Colloids toward Green Chemistry. *ACS Nano* **2016**, *10*, 5550−5559.

(15) Rives, V. *Layered Double Hydroxides: Present and Future*; Nova Science Publishers, Inc.: New York, 2001.

(16) Gash, A. E.; Tillotson, T. M.; Satcher, J. H., Jr.; Poco, J. F.; Hrubesh, L. W.; Simpson, R. L. Use of Epoxides in the Sol−Gel Synthesis of Porous Iron(III) Oxide Monoliths from Fe(III) Salts. *Chem. Mater.* **2001**, *13*, 999−1007.

(17) Yanagisawa, T.; Shimizu, T.; Kuroda, K.; Kato, C. The Preparation of Alkyltrimethylammonium-Kanemite Complexes and Their Conversion to Microporous Materials. *Bull. Chem. Soc. Jpn.* **1990**, *63*, 988−992.

(18) Kresge, C. T.; Leonowicz, M. E.; Roth, W. J.; Vartuli, J. C.; Beck, J. S. Ordered Mesoporous Molecular Sieves Synthesized by a Liquid-Crystal Template Mechanism. *Nature* **1992**, *359*, 710−712.

(19) Kodas, T. T.; Hampden-Smith, M. J. *Aerosol Processing of Materials*; John Wiley & Sons: New York, 1999.




DOI: 10.1021/acs.chemmater.6b02510
*Chem. Mater.* 2016, 28, 5606−5610

(20) Hu, Z.-A.; Xie, Y.-L.; Wang, Y.-X.; Xie, L.-J.; Fu, G.-R.; Jin, X.-Q.; Zhang, Z.-Y.; Yang, Y.-Y.; Wu, H.-Y. Synthesis of $\alpha$-Cobalt Hydroxides with Different Intercalated Anions and Effects of Intercalated Anions on Their Morphology, Basal Plane Spacing, and Capacitive Property. *J. Phys. Chem. C* **2009**, *113*, 12502−12508.
(21) Wang, L.; Dong, Z. H.; Wang, Z. G.; Zhang, F. X.; Jin, J. Layered $\alpha$-$Co(OH)_2$ Nanocones as Electrode Materials for Pseudocapacitors: Understanding the Effect of Interlayer Space on Electrochemical Activity. *Adv. Funct. Mater.* **2013**, *23*, 2758−2764.
(22) Soler-Illia, G. J. A. A.; Jobbàgy, M.; Regazzoni, A. E.; Blesa, M. A. Synthesis of Nickel Hydroxide by Homogeneous Alkalinization. Precipitation Mechanism. *Chem. Mater.* **1999**, *11*, 3140−3146.
(23) Kuroda, Y.; Miyamoto, Y.; Hibino, M.; Yamaguchi, K.; Mizuno, N. Tripodal Ligand-Stabilized Layered Double Hydroxide Nanoparticles with Highly Exchangeable $CO_3^{2-}$. *Chem. Mater.* **2013**, *25*, 2291−2296.
(24) Fan, J.; Boettcher, S. W.; Stucky, G. D. Nanoparticle Assembly of Ordered Multicomponent Mesostructured Metal Oxides via a Versatile Sol-Gel Process. *Chem. Mater.* **2006**, *18*, 6391−6396.
(25) Tsung, C.-K.; Fan, J.; Zheng, N.; Shi, Q.; Forman, A. J.; Wang, J.; Stucky, G. D. A General Route to Diverse Mesoporous Metal Oxide Submicrospheres with Highly Crystalline Frameworks. *Angew. Chem., Int. Ed.* **2008**, *47*, 8682−8686.
(26) Jobbágy, M.; Regazzoni, A. E. Compositional and Structural Control on Anion Sorption Capability of Layered Double Hydroxides (LDHs). *J. Colloid Interface Sci.* **2013**, *393*, 314−318.
(27) Reboul, J.; Furukawa, S.; Horike, N.; Tsotsalas, M.; Hirai, K.; Uehara, H.; Kondo, M.; Louvain, N.; Sakata, O.; Kitagawa, S. Mesoscopic Architectures of Porous Coordination Polymers Fabricated by Pseudomorphic Replication. *Nat. Mater.* **2012**, *11*, 717−723.
(28) Okada, K.; Ricco, R.; Tokudome, Y.; Styles, M. J.; Hill, A. J.; Takahashi, M.; Falcaro, P. Copper Conversion into $Cu(OH)_2$ Nanotubes for Positioning $Cu_3(BTC)_2$ MOF Crystals: Controlling the Growth on Flat Plates, 3D Architectures, and as Patterns. *Adv. Funct. Mater.* **2014**, *24*, 1969−1977.
(29) Huang, M.; Zhang, Y.; Li, F.; Zhang, L.; Ruoff, R. S.; Wen, Z.; Liu, Q. Self-Assembly of Mesoporous Nanotubes Assembled from Interwoven Ultrathin Birnessite-type $MnO_2$ Nanosheets for Asymmetric Supercapacitors. *Sci. Rep.* **2014**, *4*, 3878.
(30) Liu, Z.; Yu, A.; Lee, J. Y. Synthesis and Characterization of $LiNi_{1-x-y}Co_xMn_yO_2$ as the Cathode Materials of Secondary Lithium Batteries. *J. Power Sources* **1999**, *81*−*82*, 416−419.
(31) Ma, F.; Ou, Y.; Yang, Y.; Liu, Y.; Xie, S.; Li, J.-F.; Cao, G.; Proksch, R.; Li, J. Nanocrystalline Structure and Thermoelectric Properties of Electrospun $NaCo_2O_4$ Nanofibers. *J. Phys. Chem. C* **2010**, *114*, 22038−22043.
(32) Oliva, P.; Leonardi, J.; Laurent, J. F.; Delmas, C.; Braconnier, J. J.; Figlarz, M.; Fievet, F.; Guibert, A. Review of the Structure and the Electrochemistry of Nickel Hydroxides and Oxy-Hydroxides. *J. Power Sources* **1982**, *8*, 229−255.
(33) Feng, L.; Zhu, Y.; Ding, H.; Ni, C. Recent Progress in Nickel Based Materials for High Performance Pseudocapacitor Electrodes. *J. Power Sources* **2014**, *267*, 430−444.
(34) Zheng, J. P.; Jow, T. R. A New Charge Storage Mechanism for Electrochemical Capacitors. *J. Electrochem. Soc.* **1995**, *142*, L6−L8.
(35) Lu, Q.; Chen, J. G.; Xiao, J. Q. Nanostructured Electrodes for High-Performance Pseudocapacitors. *Angew. Chem., Int. Ed.* **2013**, *52*, 1882−1889.



DOI: 10.1021/acs.chemmater.6b02510
*Chem. Mater.* 2016, 28, 5606−5610